

# Spectromicroscopy at the XM-1

Greg Denbeaux<sup>1,2</sup>, Lewis Johnson<sup>1</sup>, Werner Meyer-Ilse<sup>1</sup>

<sup>1</sup>*Center for X-ray Optics, LBNL, Berkeley, CA 94720*

<sup>2</sup>*Duke University, Free Electron Laser Lab, Durham, NC 27708*

**Abstract.** The XM-1 x-ray microscope was built to obtain high-resolution transmission images from a wide variety of thick ( $< 10$  micron) samples. Modeled after a conventional full-field microscope, XM-1 makes use of zone plates for the condenser and objective elements. Recent work has enabled the microscope to be used for spectroscopic imaging as well. The bandwidth of light on the sample is limited by a linear monochromator which is formed by the combination of a condenser zone plate (CZP) and a pinhole at the sample plane. This combination gives a good spectral resolution which has been measured to be  $\lambda/\Delta\lambda = 700$ . This is high enough to be able to distinguish between different elements and even some chemical states on the same scale as the spatial resolution of the instrument which is 36 nm. The measured spectral resolution and the calculated spectral resolution will both be shown.

## INTRODUCTION

The XM-1 x-ray microscope is a full field imaging microscope (1). Radiation produced by a bending magnet at the Advanced Light Source (ALS) is collected by a “large” (9 mm diameter) fresnel condenser zone plate (CZP) which projects the light through a pinhole and illuminates the sample. The photon energy which illuminates the sample can be changed within 250 and 900 eV. The light that passes through the sample is imaged through a high precision objective micro zone plate (MZIP) (45  $\mu\text{m}$  diameter) and magnified onto a CCD camera. The field of view of the microscope is 10  $\mu\text{m}$  with a spatial resolution of 36 nm.

The monochromator is composed of the CZP and a pinhole about 100  $\mu\text{m}$  from the sample plane and is used to control the sample illumination wavelength. Zone plates have chromatic aberrations, so a change in the distance between the CZP and the sample changes the energy which is focused onto the sample plane. In order to uniformly illuminate the object, the CZP is uniformly scanned to fill the area being imaged. Since the spectral resolution is highest at the center of the spot from the CZP, reducing the area of the CZP scanning motion increases the spectral resolution with a corresponding decrease in the field of view. The pinhole is at a location very near to the sample plane compared to the CZP to sample plane distance (200 mm), so the aperture of the monochromator system is often limited by the size of the sample plane being imaged. The main function of the pinhole is to reduce background light in the system, thus improving spectral purity. During spectroscopic imaging with XM-1, the MZIP and CCD camera also move in order to form a proper image at each energy.

In order to obtain a spectrum we take multiple full field images, each at a different photon energy. Each image is a two dimensional array representing the transmitted photon flux through the sample. The combined data set stacks the individual images along an axis representing photon energy. As long as each image is aligned to within the spatial resolution, then the spectra for each single pixel of the image is found in the energy direction of the data set. This alignment can be difficult, as there can be unwanted off axis motion from the movement of the MZP and CCD. This motion could cause a shift in the projected image on the CCD camera.

## **IMAGE ALIGNMENT**

In order to combine imaging with spectral information, each image at different energies must be aligned. Then each pixel in the series of images at different energies represents the spectral information at that location of the image. Images at different energies with XM-1 require motion of the micro zone plate along the optical axis to properly focus at the chosen energy. The motion of the MZP allows for the possibility of a component of the motion to be transverse to the optical axis and cause a corresponding shift to the image relative to the previous image. Two ways to compensate for this are to use the autocorrelation of the images to determine the relative shift between them or to measure the actual shift of the micro zone plate relative to the optical axis. For either of these methods, software can be used to automatically shift each image into alignment. The autocorrelation method can be used without any additional hardware, but the images need to contain distinct features for the method to work properly. A lightly absorbing sample without distinct features may not always align properly using this technique. In order to avoid this problem, four capacitive micrometers were installed on XM-1 to accurately measure the location of the MZP. With this information, subsequent images could be automatically shifted into alignment with software. The system was designed to measure the location of the MZP to within an accuracy of a few nanometers, but initial calibrations of the system have only been accurate to within 70nm rms. Further testing and calibration should be able to reduce this error to better than the spatial resolution of 36nm.

## **CALCULATED SPECTRAL RESOLUTION**

A numerical simulation was performed to calculate the expected spectral resolution of our system. We have assumed that the CZP has no aberrations other than the known chromatic aberrations, and that the bending magnet illumination is spatially incoherent. These calculations have been performed with no scanning of the CZP. The CZP-to-sample distance was set at 200 mm for which the energy in focus at the sample plane is 500 eV. The condenser zone plate has 41,000 zones and a 9-mm diameter. There is a 3-mm diameter central stop which obstructs the undiffracted light from reaching the sample.

The convolution of the point spread function of the XM-1 condenser zone plate with the source distribution from the ALS bending magnet yields the field distribution at the sample. The nominal size of the ALS source at the bend magnet is  $\sigma = 53 \mu\text{m}$  horizontal and  $\sigma = 44 \mu\text{m}$  vertical (2). For a given wavelength,  $\lambda$ , the lens plane field at a point  $(x, y)$  from a point source in the source plane with coordinates  $(\varepsilon, \eta)$  is (3,4):

$$u(x, y; \varepsilon, \eta) = \frac{1}{i\lambda z_1} \exp\left(\frac{ik}{2z_1}[(x - \varepsilon)^2 + (y - \eta)^2]\right) \quad (1)$$

Where  $z_1$  is the distance from the source to the CZP lens, 17 meters, and the wavenumber,  $k$ , is  $2\pi/\lambda$ . Just past the lens plane, the field of the CZP can be modeled as a simple thin lens:

$$u'(x, y; \varepsilon, \eta) = u(x, y; \varepsilon, \eta)P(x, y) \exp\left(\frac{-ik}{2f}(x^2 + y^2)\right) \quad (2)$$

Where the annular pupil function  $P(x, y)$  is 1 between the central obstruction (3 mm diameter) and the lens aperture (9 mm diameter) and is 0 elsewhere. The exponential term is the impulse response of a lens with focal length,  $f$ . The field at the image plane  $(u, v)$  due to a point source at the source plane is given by the convolution of  $u'$  with the point spread function of free space.

$$u_{\text{image}}(u, v; \varepsilon, \eta) = \frac{1}{i\lambda z_2} \iint u'(x, y; \varepsilon, \eta) \exp\left(\frac{ik}{2z_2}[(u - x)^2 + (v - y)^2]\right) dx dy \quad (3)$$

where  $z_2$ , the distance from the lens to the image plane, is 200 mm for this calculation. The convolution with the source can be performed with numerical integration techniques for a series of different photon energies and corresponding different focal lengths from the CZP. The result of these calculations is the illumination at the sample plane for each photon energy. Figure 1 shows the calculated spectral distribution of the illumination near 500 eV on the sample, averaged over areas of  $4 \mu\text{m}^2$ ,  $9 \mu\text{m}^2$  and  $16 \mu\text{m}^2$ . Using  $\Delta E$  as the FWHM of these distributions, the spectral resolution calculations yield  $E/\Delta E = 1400$  within a  $4 \mu\text{m}^2$  spot,  $E/\Delta E = 900$  within a  $9 \mu\text{m}^2$  spot, and  $E/\Delta E = 700$  within a  $16 \mu\text{m}^2$  spot. Since the best spectral resolution is located at the center of the CZP spot on the sample, the choice of a small area CZP scan sacrifices the field of view for high spectral resolution.

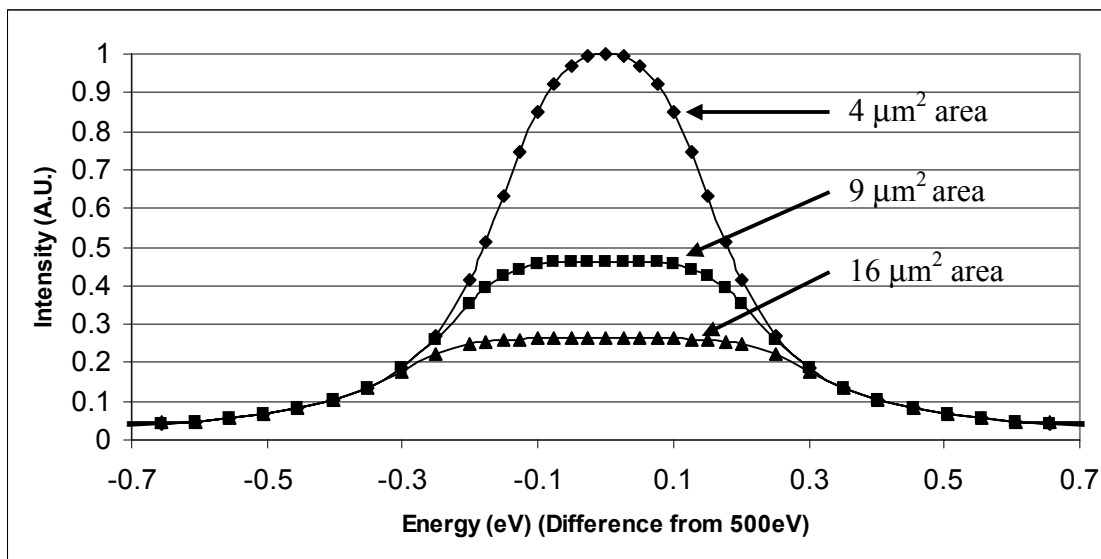


**Figure 1.** Average intensities at energies near 500 eV for 4  $\mu\text{m}^2$ , 9  $\mu\text{m}^2$ , and 16  $\mu\text{m}^2$  areas.

## MEASURED SPECTRAL RESOLUTION

The measured spectrum of a sample in an instrument is given by the convolution of the actual sample spectrum with the instrument bandwidth. The spectrum of a thin sample of  $\text{CaF}_2$  at the calcium L edge ( $\sim 350$  eV) was measured in both XM-1 and the Calibration and Standards Beamline (6.3.2) at the ALS. The Calibration and Standards beamline has a measured spectral resolution of  $E/\Delta E$  greater than 4000 (5). The absorption in XM-1 was measured over a 9  $\mu\text{m}^2$  imaging area. Both the measured spectrum of  $\text{CaF}_2$  from XM-1 and from 6.3.2 are shown in Figure 2.

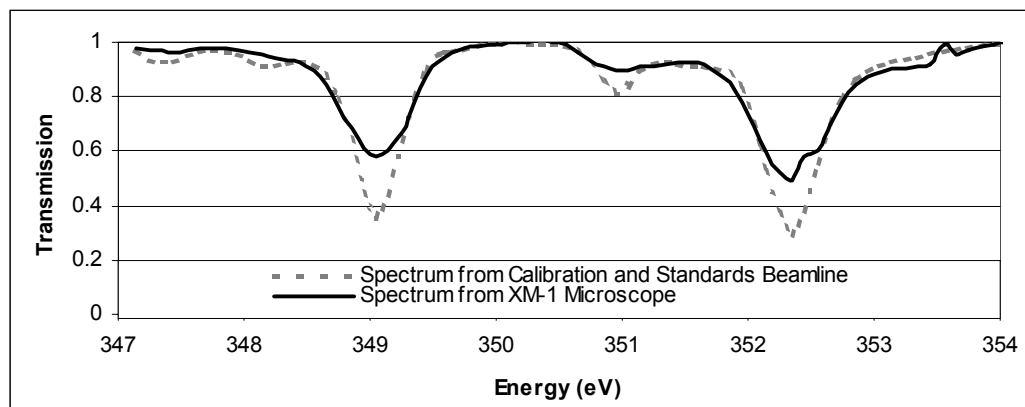


**Figure 2.** Measured Spectra of  $\text{CaF}_2$  by XM-1 microscope and Calibration and Standards Beamline, 6.3.2.

The distribution of the bandwidth of XM-1 was simulated with a gaussian distribution and was convolved with the high spectral resolution data from the Calibration and Standards Beamline. The parameters of the gaussian distribution were adjusted until the result of the convolution very nearly matched the measured spectrum from XM-1. The result was a distribution which has a FWHM of 0.5 eV at 350 eV. This yields a measured spectral resolution for XM-1 for this  $9\text{ }\mu\text{m}^2$  field of view is  $E/\Delta E = 700$ . This is comparable to the  $E/\Delta E = 900$  which was calculated for this field of view. Such bandwidth is sufficient to distinguish between different elements and some chemical states on the spatial resolution of the microscope.

## RESULTS

We have observed absorption peaks from the K edges of C,N,O and the L edges of Ca,Ti,V,Cr,Mn,Fe. An example of the absorption features that we have observed is shown in Figure 3. This is the absorption for chromium in three different oxidation states. The increase in oxidation state increases the binding energy and can be seen by the shift to higher energy of the absorption peaks.

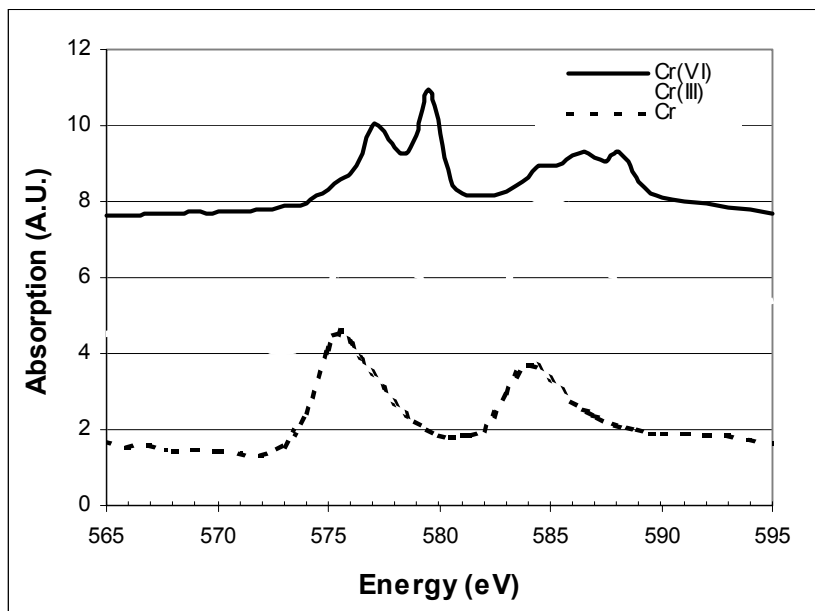


**Figure 3.** Spectra from Cr,  $\text{Cr}^{3+}$ , and  $\text{Cr}^{6+}$ . The shift in energies of the peak absorption is large enough to be distinguished with this spectral resolution.

$\text{Cr}^{6+}$  compounds are often soluble and toxic while  $\text{Cr}^{3+}$  compounds are typically insoluble and therefore not as toxic. There are bacteria which are known to reduce the more toxic  $\text{Cr}^{6+}$  to the less toxic  $\text{Cr}^{3+}$ , but there is a lot not known about the process. The combination of a high spatial resolution of 36 nm with the spectroscopic resolution capable of distinguishing the different chemical species will allow us to address this in future research.

The combined capabilities of a high spatial resolution of 36 nm, moderate spectral resolution of  $\lambda/\Delta\lambda = 700$ , and the ability to image thick, wet samples makes XM-1 a unique tool for many scientific applications. We plan to continue to develop and to actively exploit these features in the future.

## ACKNOWLEDGMENTS

The authors would like to acknowledge our colleagues of the Center for X-ray Optics, the Life Science Division, and the ALS, especially D. T. Attwood, E. Gullikson, K. Goldberg, and P. Naulleau. This work is funded by the U.S. Dept. of Energy office of Basic Energy Science, the U.S. Navy, Office of Naval Research under grant N00014-94-1-0818 and the U.S. Army Research office under grand DAAH04-96-1-0246. This great instrument is a testament to the hard work, dedication, and insight of Werner Meyer-Ilse. His driving force and light will be deeply missed.

## REFERENCES

1. Meyer-Ilse, W., et. al., "The High Resolution X-Ray Microscope, XM-1," to be published in these proceedings.
2. Private communication with H. Padmore (ALS).
3. Goodman, J., *Introduction to Fourier Optics*, New York: McGraw-Hill, 1996.
4. Born, M., and Wolf, E., *Principles of Optics*, Cambridge: Cambridge University Press, 1980.
5. Underwood, J.H., et al., "High-resolution, high-flux, user friendly VLS beamline at the ALS for the 50-1300eV energy region," *Journal of Electron Spectroscopy and Related Phenomena*, **92**, 265-272 (1998).